International Journal of Pharmaceutics 400 (2010) 221–233

Contents lists available at ScienceDirect

International Journal of Pharmaceutics

journal homepage: www.elsevier.com/locate/ijpharm

Pharmaceutical Nanotechnology

Antitumor activity of quaternized chitosan-based electrospun implants against Graffi myeloid tumor

R. Toshkova [a], N. Manolova [b,*], E. Gardeva [a], M. Ignatova [b], L. Yossifova [a], I. Rashkov [b,*], M. Alexandrov [a]

[a] Institute of Experimental Pathology and Parasitology, Bulgarian Academy of Sciences, Acad. G. Bonchev St. bl. 25, BG-1113 Sofia, Bulgaria
[b] Laboratory of Bioactive Polymers, Institute of Polymers, Bulgarian Academy of Sciences, Acad. G. Bonchev St. bl. 103A, BG-1113 Sofia, Bulgaria

ARTICLE INFO

Article history:
Received 18 June 2010
Received in revised form 12 August 2010
Accepted 25 August 2010
Available online 9 September 2010

Keywords:
Antitumor activity
Chitosan
Electrospinning
Drug delivery system
Nanofibrous implants
Doxorubicin

ABSTRACT

Nanofibrous implants containing quaternized chitosan (QCh), poly(L-lactide-co-D,L-lactide) (coPLA), and the antitumor drug doxorubicin (DOX) were fabricated by electrospinning. The surface chemical composition and the morphology of the implants were characterized by XPS and SEM. *In vitro* cell viability studies demonstrated that QCh- and DOX-based implants exhibited high cytotoxicity against Graffi tumor cells. The implants efficiently inhibited the growth of Graffi tumor in hamsters with minimum weight loss. Insertion of QCh/coPLA/DOX implants in the place of removed tumor led to an increase in the animal survival rate and to a decrease in the percentage of recurrences.

1. Introduction

The nonspecific systematic distribution of the antitumor drugs and the low concentration of the drug at the tumor site are the main disadvantages of the conventional tumor chemotherapy. One promising approach to overcome these drawbacks is the localized and controlled delivery of antitumor drugs using polymer systems implanted in the tumor tissue. The advantages of this method are not only the achievement of a high local concentration of an antitumor drug by using a small amount of drug, but also reducing toxicity, reducing the frequency of drug administrations, and providing convenience (Liu et al., 2001). Moreover, the local sustained release of an antitumor drug provides an increase in the duration of tumor exposure to the drug. Over the last decade, among the polymer systems for controlled drug release those based on biodegradable synthetic and natural polymers have been most extensively utilized (Liu et al., 2001; Xu et al., 2006; Xiangyang et al., 2007; Hu et al., 2009).

Electrospinning is a cutting edge technology for producing continuous polymer fibers with diameters ranging from a few nanometers to several micrometers (Reneker and Chun, 1996), that has recently attracted attention in the field of drug delivery. The use of non-woven textile composed of electrospun micro- and nanofibers as antitumor drug carriers is a promising approach for the targeted delivery of antitumor drugs, especially in postoperative local chemotherapy, because of their expected advantages, such as improved therapeutic effect, reduced toxicity and convenience.

The natural polysaccharide chitosan is particularly promising as drug carrier because of its set of valuable properties such as biodegradability, non-toxicity and presence of reactive functional groups (Janes et al., 2001; Han et al., 2008; Park et al., 2010). Chitosan and its quaternized derivatives (QCh) are reported to possess good antitumor activity, as well as good antimicrobial and antimycotic properties (Kim et al., 1997; Qin et al., 2002; Rabea et al., 2003; Huang et al., 2006). Previously, we have reported that the preparation of nanofibers of QCh by electrospinning of its aqueous solutions is feasible only in the presence of a second non-ionogenic polymer, e.g. poly(vinyl alcohol) or poly(vinyl pyrrolidone) (Ignatova et al., 2006, 2007). Recently, we have shown that electrospinning of mixed solutions of QCh and poly(L-lactide-*co*-D,L-lactide) (coPLA) in a common solvent allows one-step preparation of hybrid nanofibrous materials, that combine the antimicrobial properties of QCh and the good physico-mechanical properties of the aliphatic polyesters (Ignatova et al., 2009). It has been found that after incorporation of QCh in the electrospun mats, they acquire antimicrobial and antimycotic activity (Ignatova et al., 2006, 2007, 2009).

As a model antitumor drug doxorubicin hydrochloride (DOX) (Scheme 1) is chosen in the present study since it possesses broad spectrum antitumor activity and because of its widely use in the clinical field in the treatment of tumor diseases of the breast, cervix,

* Corresponding authors. Tel.: +359 2 9793289; fax: +359 2 8700309.
E-mail addresses: manolova@polymer.bas.bg (N. Manolova), rashkov@polymer.bas.bg (I. Rashkov).

0378-5173/$ – see front matter © 2010 Elsevier B.V. All rights reserved.
doi:10.1016/j.ijpharm.2010.08.039

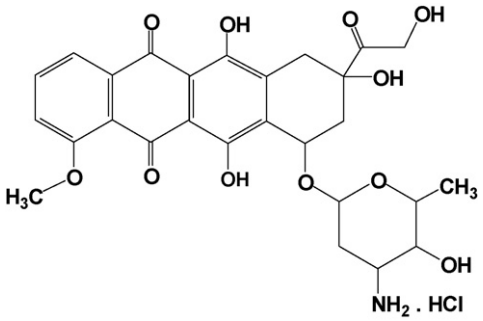

Scheme 1. Structure of doxorubicin hydrochloride (DOX).

liver and colon, as well as leukemia (Freedman et al., 1980; Crown et al., 2002; Prahalathan et al., 2006). It is known however, that when it is applied at therapeutic concentrations, severe side effects are observed, such as cytotoxicity in normal tissue, pervasive cardiotoxic effects, and inherent multidrug resistance effect, which further limit its therapeutic efficacy. Recently, we have demonstrated that QCh-containing nanofibrous electrospun materials and those in which DOX has been physically entrapped exhibit *in vitro* antitumor activity against HeLa human cervical cancer cell line (Ignatova et al., 2010). To the best of our knowledge, until now, no data about *in vitro* and *in vivo* antitumor activity of QCh- and DOX-containing nanofibrous materials against Graffi myeloid tumor have been reported. Studies directed towards the assessment of the antitumor efficacy of electrospun materials from (co)polymers of lactic acid-containing antitumor drugs for local tumor treatment are still scarce (Ranganath and Wang, 2008).

The present study demonstrates the possibility of fabricating nanofibrous implants based on QCh, coPLA and/or DOX. These implants have been characterized by scanning electron microscopy (SEM) and X-ray photoelectron spectroscopy (XPS). Their *in vitro* cytotoxicity against Graffi cells has been evaluated. Two sets of *in vivo* experiments have also been performed. In the first set of experiments nanofibrous implants have been placed directly into a specially made incision in the animal tumor and in the second set of experiments after the tumor extirpation the implants have been inserted into the tumor site. The biometrical parameters of the tumor growth in the presence of implants, as well as the changes in the tumor tissue evidenced by the data from histological studies have also been reported.

2. Materials and methods

2.1. Materials

Formaldehyde solution (~36% in water) (Fluka), $NaBH_4$ (Fluka), CH_3I (Fluka), NaI (Fluka), glutaraldehyde solution (~50% in water) (Fluka) were of analytical grade of purity and were used as received. Prior to use, *N*-methyl-2-pyrrolidone (NMP) (Fluka) was freshly distilled under reduced pressure. Dimethylformamide (DMF) (Fluka) and dimethyl sulfoxide (DMSO) (Fluka) were dried with molecular sieves (4 Å) prior to use. Poly(L-lactide-*co*-D,L-lactide) – Resomer® LR 708 (coPLA) ($\overline{M}_w$ 911 000 g mol^{-1}, $\overline{M}_w/\overline{M}_n = 2.46$) – (molar ratio L-lactide: D,L-lactide = 69:31) was kindly provided as a gift from Boerhinger-Ingheleim Chemicals Inc (Germany). Chitosan with a molecular weight of 380 000 g/mol (Aldrich) and a degree of deacetylation 80% was used. DOX was purchased from Sigma–Aldrich. For the *in vitro* experiments DOX was initially dissolved in ethanol at a concentration of the stock solution 3 mg/mL and further was dissolved in DMEM at the concentrations of 10, 50, 100 and 200 μg/mL. For the *in vivo* experiments DOX was dissolved in sterile PBS at the concentrations of 5 and 10 mg/kg. Propidium iodide (PI) and acridine orange (AO) were obtained from Sigma Chemical (St. Louis, MO). The concentration of the stock solutions of PI and AO was 1 mg/mL in PBS.

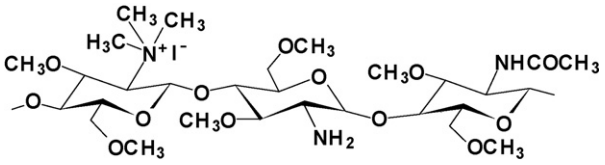

Scheme 2. Quaternized chitosan (QCh) chain sequence.

2.2. N,N,N-Trimethyl chitosan iodide—synthesis and characterization

A quaternized chitosan derivative (QCh) (Scheme 2)—*N*,*N*,*N*-trimethyl chitosan iodide was synthesized according to a known procedure (Kim et al., 1997). Briefly, in the first step *N*-methyl chitosan was prepared by reacting chitosan and formaldehyde via Schiff's base intermediate and subsequent hydrogenation with $NaBH_4$. The product was purified from unreacted aldehyde and inorganic products by Soxhlet-extraction with ethanol and diethylether for 4 days. The obtained *N*-methyl chitosan was filtered out and vacuum-dried at 40 °C for 2 days. Yield—94%. The resulting *N*-methyl chitosan was quaternized using methyl iodide. *N*,*N*,*N*-trimethyl chitosan iodide was purified by twofold precipitation in acetone and dried under reduced pressure at 40 °C. Yield—96%.

The quaternization degree of QCh was determined using two independent methods: ^{1}H NMR spectroscopy (Bruker spectrometer, 400.13 MHz, D_2O, 333 K) and potentiometric titration of the iodide form with aqueous silver nitrate, using a working silver electrode and a reference calomel electrode. The quaternization degree was calculated from the intensity ratio of the signal at 3.12 ppm for $-N^+-(C\underline{H}_3)_3I^-$ to that of H-1. This value (70%) is in very good agreement with the quaternization degree determined potentiometrically (72%). The degree of methylation of –OH functions was determined from the intensity ratios of the signal of $C\underline{H}_3$–O at 3.51 and 3.38 ppm, for OH at C-3 and C-6 position, respectively, and the H^1 signal. The degree of methylation of H^3 and H^6 was both 98%.

2.3. Preparation of pristine and DOX-containing QCh/coPLA and coPLA nanofibers by electrospinning

coPLA nanofibers were obtained by electrospinning of coPLA solutions in dry DMF/DMSO (60/40, v/v; coPLA concentration of 5 wt.%). DOX-containing coPLA mats were obtained by electrospinning of coPLA/DOX mixed solutions (3% and 6% DOX in weight percent to coPLA content) in dry DMF/DMSO (60/40, v/v) at polymer concentration of 5 wt.%. QCh/coPLA nanofibers at weight ratio of QCh/coPLA = 30:70 were obtained by electrospinning of their mixed solutions in dry DMF/DMSO (60/40, v/v) at total polymer concentration of 5 wt.%. DOX-containing QCh/coPLA mats were prepared by electrospinning of mixed QCh/coPLA solutions (weight ratio of QCh/coPLA = 30:70) containing DOX (3% and 6% in weight percent to QCh/coPLA content) in dry DMF/DMSO (60/40, v/v) at total polymer concentration of 5 wt.%. The mixed solutions were placed in a plastic 5 mL syringe equipped with a 20 G needle. The positive lead of a direct current (DC) high voltage power supply was connected to the needle via alligator clips. The rotating, grounded drum with a diameter of 45 mm, was placed 18 cm from the needle tip, and the rotating speed was maintained at 1100 rpm. The spinning solution was delivered using a syringe pump at a controlled feed rate of 1.0 mL/h at a constant value of the applied voltage (25 kV). The

electrospun fibrous mats were placed under vacuum overnight at 40 °C to remove any solvent residues.

Prior to electrospinning, the dynamic viscosity of the spinning solutions was measured using a Brookfield LVT viscometer equipped with a small-sample thermostated adapter, spindle and chamber SC4-18/13R, at 25 ± 0.1 °C. The electrical resistance of the spinning solutions was measured in an electrolytic cell equipped with rectangular sheet platinum electrodes having a surface area of 0.6 cm^2 and disposed at a distance of 2.0 cm. During the measurements short electric pulses with opposite direction were applied to the Pt electrodes in order to avoid accumulation of ionic charge and polarization effects in the vicinity of the electrode surface. This allowed solution resistance in the range of 20–2000 kΩ to be measured with an accuracy of ±3%. Calibration of the electrolytic cell was performed using a standard solution of KCl (conductivity 140.8 mS/m) and the cell constant (K_{cell}) was determined. The conductivity of the spinning solutions (σ, μS/cm) was calculated from the following equation:

$$\sigma = \frac{1}{\rho} = \frac{1}{K_{cell} \cdot R} \quad (1)$$

where ρ is the specific resistance of the solution (μΩ cm), R—electrical resistance of the solution (μΩ).

2.4. Preparation of nanofibrous implants

Pristine and DOX-containing nanofibrous discs were obtained by punching the fiber mats into discs with three different diameters (d = 5, and 13 mm for *in vitro* studies and 10 mm for *in vivo* studies). Implants in the form of nanofibrous tablets were prepared from the nanofibrous discs in a SPECAC manually operated hydraulic press (SPECAC LTD., London, England) with compression of 5 MPa.

Photographs of implants are shown in Fig. 1. The color of coPLA implants was white and that of QCh/coPLA implants was pale yellow. The incorporation of DOX in the implants led to a change of their color to red. The implants were sterilized using ^{60}Co gamma irradiation at a dose of 15 kGy before using for *in vitro* and *in vivo* studies.

2.5. Characterization of the implants

The morphology of the fibrous implants was studied by SEM. The implants were vacuum-covered with carbon and gold and observed by a Philips 515 scanning electron microscope. The average fiber diameter and the standard deviation were estimated in terms of the criteria for complex evaluation of electrospun materials (Spasova et al., 2006) using Image J software (Rasband, 2006). At least 30 randomly selected fibers from each SEM micrograph were measured.

The elemental composition of the surface of electrospun pristine and DOX-containing implants was determined by X-ray photoelectron spectroscopy (XPS). The XPS measurements were carried out in the UHV chamber of an ESCALAB-MkII (VG Scientific) electron spectrometer using Mg Kα excitation with a total instrumental resolution of ~1 eV. Energy calibration was performed, taking the C_{1s} line at 285 eV as a reference. Surface atomic concentrations were evaluated using Scofield's ionization cross-sections with no corrections for λ (the mean free path of photoelectrons) and the analyzer transmission function. The experimental values for the element atomic percentages obtained from XPS analysis are the average of three independent measurements.

In order to demonstrate the presence of DOX in the DOX-containing implants, they were analyzed by fluorescence microscopy (Leika DM 500B, Wetzlar, Germany). For the sake of comparison, the pristine coPLA and QCh/coPLA implants were also observed by fluorescence microscope.

2.6. In vitro experiments

Primary Graffi cells isolated from the solid myeloid tumor tissue from golden Syrian hamsters under aseptic conditions were cultured in RPMI-1640 medium containing 10% fetal heat-inactivated serum, 2 mM glutamine and 100 μg/mL penicillin–streptomycin. The cells were maintained at 37 °C in a humidified incubator containing 5% CO_2. All culture reagents were purchased from Gibco/BRL (Grand Island, NY).

The cytotoxicity of DOX against Graffi tumor cells was assessed *in vitro* by the MTT staining method as described by Mossmann (1983). Graffi cells (2×10^4 cells/well) in RPMI-1640 containing 10% FBS were seeded into 96-well flat bottom culture plates for 24 h. After that the cells were washed with fresh medium and were treated with different DOX concentrations (10, 50, 100 and 200 μg/mL) or implant formulations for various periods of time (24 h for DOX-treatment and 24, 48 and 72 h for implant-treatment). At the end of the treatment, the culture medium in each well was discarded and 100 μL of the MTT solution (3-(4,5-dimethylthyazol-2-yl)-2,5-diphenyl tetrazolium bromide) at a concentration of 0.5 mg/mL were added to each well followed by further incubation for 4 h at 37 °C. Formazan crystals were dissolved in 100 μL of DMSO and ethanol solution (DMSO:ethanol = 1:1). The absorbance was recorded using an ELISA reader at a wavelength of 570 nm. Doxorubicin IC_{50} was determined as a doxorubicin concentration showing 50% cell growth inhibition as compared with control cell growth. The viability of treated cells is presented as the percentage of viable control cells at different time points relative to the viability of control cells (non-treated cells), which is indicated as 100% viability.

Graffi tumor cells treated with nanofibrous implant formulations and untreated cells (control) were visualized by double staining with acridine orange (AO) and propidium iodide (PI) according to the method described by Wahab et al. (2009). Graffi cells were plated at density of 5×10^4 cells/mL on nanofibrous implants with a diameter of 13 mm in 24-well plates and incubated for 24 h in a CO_2-incubator. After 24 h of incubation nanofibrous

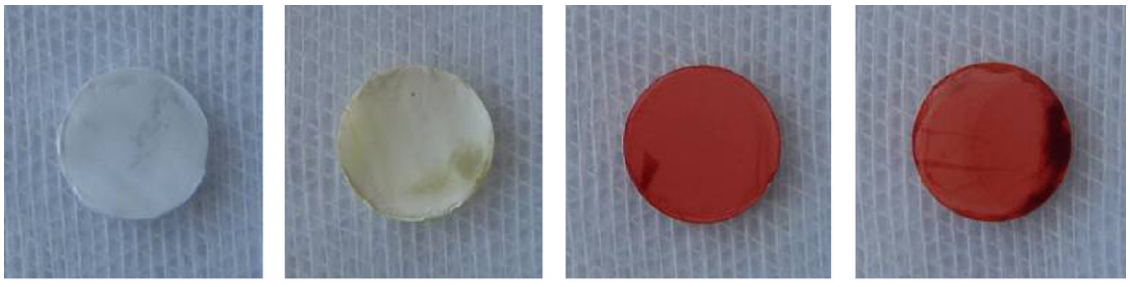

Fig. 1. Photographs of implants of coPLA (A), QCh/coPLA (B), coPLA/DOX (C), and QCh/coPLA/DOX (D).

implants were washed twice with PBS and were stained by addition of equal volumes of AO (10 μg/mL) and PI (10 μg/mL). Then they were mounted on a microscope slide under glass cover slips and were examined immediately under the fluorescence microscope (Leika DM 500B, Wetzlar, Germany). Images were recorded using a connected digital camera. At least 100 cells were counted.

2.7. In vivo experiments

Golden Syrian hamsters, 2–4 months old, weighing approximately 100 g were purchased from a breeding base Oncology Center, Sofia. The animals were kept under standard conditions in individual plastic cages with free access to food and water. All studies were performed in accordance with the Guide for Care and Use of Laboratory Animals, as proposed by the Committee on Care Laboratory Animal Resources, Commission on Life Sciences and National Research Council, and a work permit No. 11130006.

An experimental Graffi myeloid tumor was created and maintained monthly *in vivo* by subcutaneous transplantation of live tumor cells (2×10^6/mL PBS) in the interscapular area of hamsters (Toshkova et al., 2008). Between the 10th and the 15th day after tumor transplantation on the back of the hamster a solid subcutaneous tumor appeared, which progressively increased in size and after about 30 days caused death of experimental animals. Spontaneous regression in this experimental tumor model was not observed.

Primary culture of Graffi tumor cells—Briefly, the tumor tissue was isolated from hamsters with well-developed subcutaneous tumor in a standard way under aseptic conditions. It was cleared of necrotic masses and disaggregated mechanically, washed repeatedly and each time the supernatant was aspirated after centrifugation of the cells in cold centrifuge. Obtained cells are counted with a Trypan blue dye and led to the desired concentration—2×10^5 cells/mL of live tumor cells for *in vitro* experiments and 5×10^4 cells/mL for *in vivo* experiments.

5×10^4 live tumor cells per animal were transplanted subcutaneously (sc) on hamsters in the interscapular area, after applying a local anesthesia with 10% Lidocain (Lidocain spray, Egis Pharmaceuticals PLC, Budapest, Hungary). The dose of the tumor cells was optimized so that between the 10th and the 15th day after inoculation experimental animals developed well-formed solid tumor formations with a size 5–10 mm, on which two sets of experiments were conducted. In the first set of surgical trials experimental animals were selected to have well-formed tumor formations (diameter 5–10 mm) and were divided into groups of eight hamsters. Intratumor implantation of the studied variants of nanofibrous implants was carried out after surgery, providing access to tumor tissue. Hamsters were numbered and distributed in separate plastic cages. The total DOX content in the implants was 1.4 mg. The biometric parameters of tumor growth—tumor volume, animal survival rate and histopathological changes in the tumor after implantation of different implants were studied. The size of tumors was measured using a caliper and tumor volumes were calculated by the formula: $V = A \cdot B^2/2$, where A—major axis; B—minor axis (Cho et al., 2009). In the second set of surgical trials after the transplantation of live tumor cells and the appearance of solid tumor formations as mentioned above, a surgical extirpation of the tumor formation was carried out with subsequent placement of the nanofibrous implants in the operative field. The biometric parameters of tumor growth, recurrence in the operative field, metastases in the operative field and regional lymph nodes were determined.

Fragments of approximately 15 mm × 15 mm tumor pieces with nanofibrous implants were selected for histopathological studies. They were obtained from animals originating from each experimental group on the 3rd and the 7th day after implantation. Immediately after the selection procedure the tumor tissues were immersed and fixed for 48 h in 4% buffered formaldehyde. Then they were embedded in paraffin, 5–8 μm sections were prepared and stained with haematoxylin–eosin according to the standard histological technique.

2.8. Statistical analysis

The data are given as the mean ± standard deviation (SD). Significance testing was performed using one-way analysis of variance (ANOVA) followed by Bonferroni's post hoc test. Values of $^{*}p < 0.05$, $^{**}p < 0.01$ and $^{***}p < 0.001$ were considered significant.

3. Results and discussion

3.1. Preparation and characterization of DOX-containing QCh/coPLA and coPLA implants

Implants from cylindrical continuous defect-free nanofibers with an average fiber diameter of 590 ± 80 nm were obtained by electrospinning of the QCh/coPLA solutions in a mixed solvent DMF/DMSO (60:40, v/v), total polymer concentration 5 wt.%, AFS 1.4 kV/cm and feeding rate of 1.0 mL/h (Fig. 2A).

In the XPS spectra of the implants the presence of C_{1s} (285.0 eV), O_{1s} (532.3 eV), N_{1s} (399.6 and 402.4 eV) and I_{3d} (618.0 and 629.5 eV) peaks was observed. Atomic percentages (53.1% C, 37.6% O, 1.3% N and 8.0% I) experimentally determined from the XPS peaks were close to the theoretical values calculated from the chemical composition of QCh/coPLA implants (49.9% C, 39.7% O, 1.4% N and 9.0% I). The C_{1s}, N_{1s} and I_{3d} spectral regions were analyzed by peak reconstruction (Fig. 2C–E). The expanded C_{1s} spectrum consisted of four peaks: at 285.0 eV assigned to –C–H or –C–C– of coPLA and of QCh and also to –C–NH_2 of QCh, at 287.0 eV to –C–O, –C–OH, –C–OCH_3 and –C–N–C═O of QCh and to –C–O of coPLA, at 288.0 eV to –O–C–O– and –N–C═O of QCh and at 289.2 eV to –O–C═O of coPLA (Fig. 2C). The detailed N_{1s} spectrum showed two components—at 399.6 eV characteristic for –N–C═O and –NH_2 and at 402.4 eV—for ammonium group (–$N^+(CH_3)_3$) from QCh (Fig. 2D). The appearance of N_{1s} peaks and I_{3d} peaks ($I_{3d5/2}$ at 618.0 eV and $I_{3d3/2}$ at 629.5 eV) (Fig. 2E) proved the presence of QCh component in the surface layer of the QCh/PLA implants.

Considerable differences were observed in the case of adding DOX to QCh/coPLA mixed solutions in DMF/DMSO (60:40, v/v). In this case, the average diameter of the obtained fibers constituting the implants was 310 ± 50 nm (Fig. 2F). The obtained results are in accordance with previous reports on decrease in the fiber diameter upon adding the low-molecular-weight organic salt DOX (Jun et al., 2003; Spasova et al., 2004; Mincheva et al., 2005; Ignatova et al., 2006). Such observations have been attributed to the increase in the conductivity of the spinning solution in the presence of an organic salt. In the case of QCh/coPLA implant no fluorescence was detected (Fig. 2B), while QCh/coPLA/DOX implants showed fluorescence, presumably due to incorporation of DOX in the fibers (Fig. 2G). In the XPS spectra of QCh/coPLA/DOX implants (Fig. 2H–K), the peak for Cl_{2p} (198.3 eV) with the exception of the peaks for C_{1s} (285 eV), O_{1s} (532.3 eV), N_{1s} (399.5 and 402.0 eV) and I_{3d} (618.0 and 629.4 eV) was observed. The C_{1s} detailed spectrum (Fig. 2H) is deconvoluted to four peaks: at 285 eV assigned to –C–H or –C–C– of coPLA, QCh and DOX, and also to –C–NH_2 of QCh and DOX, at 286.8 eV to–C–O, –C–OH and –C–OCH_3 of QCh and DOX, to –C–O of coPLA and to –C–N–C═O of QCh, at 288.3 eV to –O–C–O– and –N–C═O of QCh and to –O–C–O– of DOX and at 289.2 eV to –O–C═O of coPLA and to –C–C═O of DOX. The detailed N_{1s} spectrum showed two components: at 399.5 eV, which was assigned to –N–C═O and –NH_2 groups of QCh and at 402.0 eV to ammonium group (–$N^+(CH_3)_3$) of QCh and to –NH_3^+ groups of DOX (Fig. 2I). A new Cl_{2p} peak was

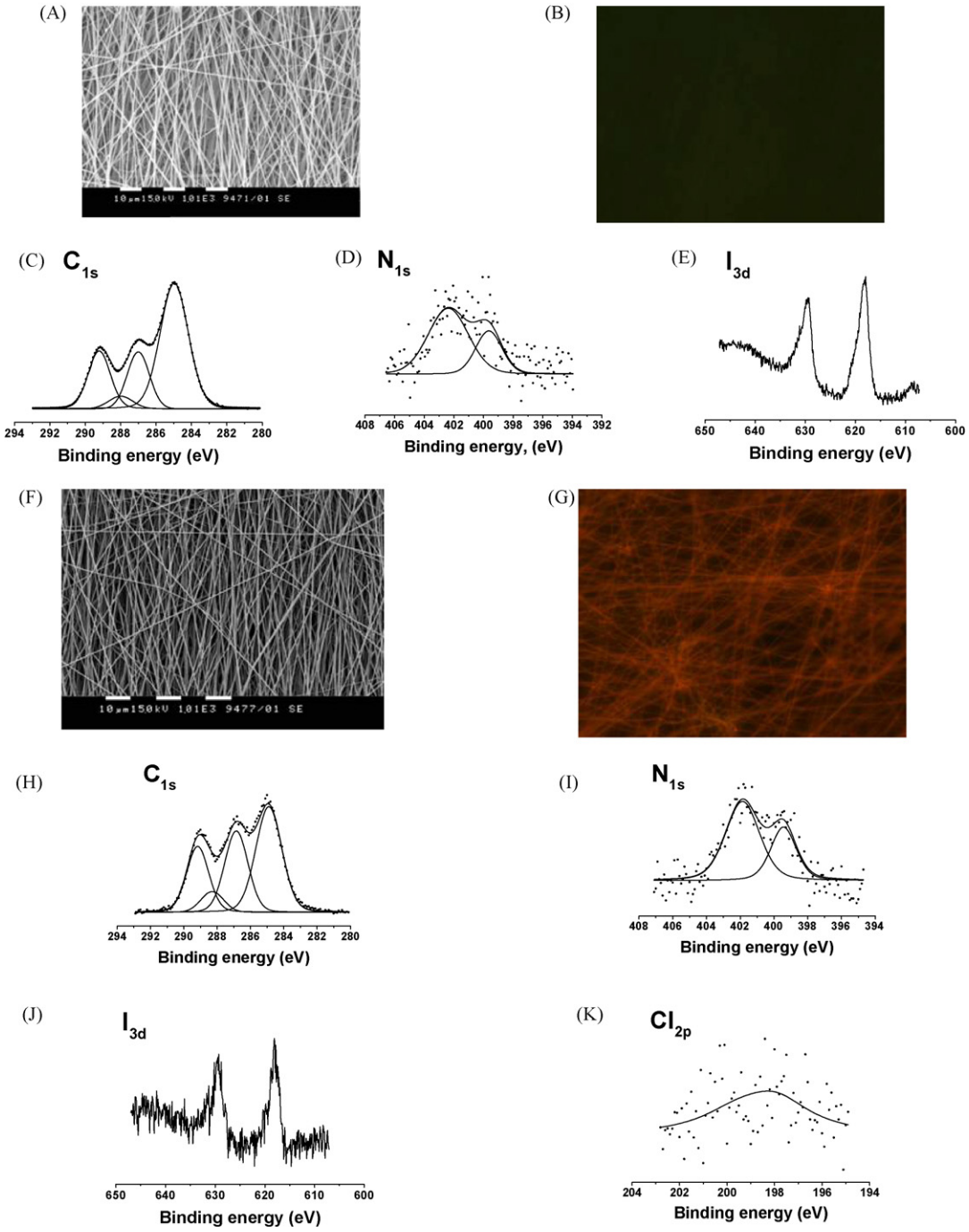

Fig. 2. SEM and fluorescence micrographs of fibrous implants: QCh/coPLA (A, B), QCh/coPLA/DOX (6 wt.% DOX) (F, G); magnification—×1000 (A, F) and ×40 (B, G). XPS peak fittings for implants of: QCh/coPLA [C_{1s} (C), N_{1s} (D) and I_{3d} (E)] and QCh/coPLA/DOX (6 wt.% DOX) [C_{1s} (H), N_{1s} (I), I_{3d} (J) and Cl_{2p} (K)].

recorded at 198.3 eV, which was attributed to the presence of DOX in the implant (Fig. 2K).

Under the above-mentioned electrospinning conditions implants from cylindrically shaped continuous coPLA fibers (average fiber diameter 830 ± 115 nm) without defects were obtained (Fig. 3A).

Fig. 3C shows the high-resolution XPS spectra in the C_{1s} region of coPLA implant. The implant presents three C_{1s} peaks. The peak at 285 eV was attributed to –C–H or –C–C–. The peak at 286.9 eV was assigned to –C–O and the peak at 288.9 eV to –O–C=O. In the detailed O_{1s} spectrum shown on the Fig. 3D, two peaks were identified. The peak at 533.3 eV was assigned to –C–O and the peak at 531.9 eV was assigned to –O–C=O. The experimentally determined atomic percentages of the elements (54.7% C and 45.3% O) were in accordance with the theoretical calculations (52.9% C and 47.1% O).

On adding DOX to coPLA solution the average fiber diameter decreased (Fig. 3E): for example, from 830 ± 115 nm to 580 ± 90 nm in the case of coPLA implant and coPLA implant containing 6 wt.% DOX, respectively. This could be accounted for the increase in the conductivity of coPLA solution from 27 to 184 μS/cm on adding the low-molecular-weight organic salt DOX. Fluorescence micrographs of pristine and DOX-containing coPLA implants are shown in Fig. 3B and F. As expected, in the case of coPLA implants there was no fluorescence, while coPLA/DOX implants showed fluorescence attributed to the incorporated DOX. The XPS broad survey spectrum for detection of major atomic species and the detailed spectra for

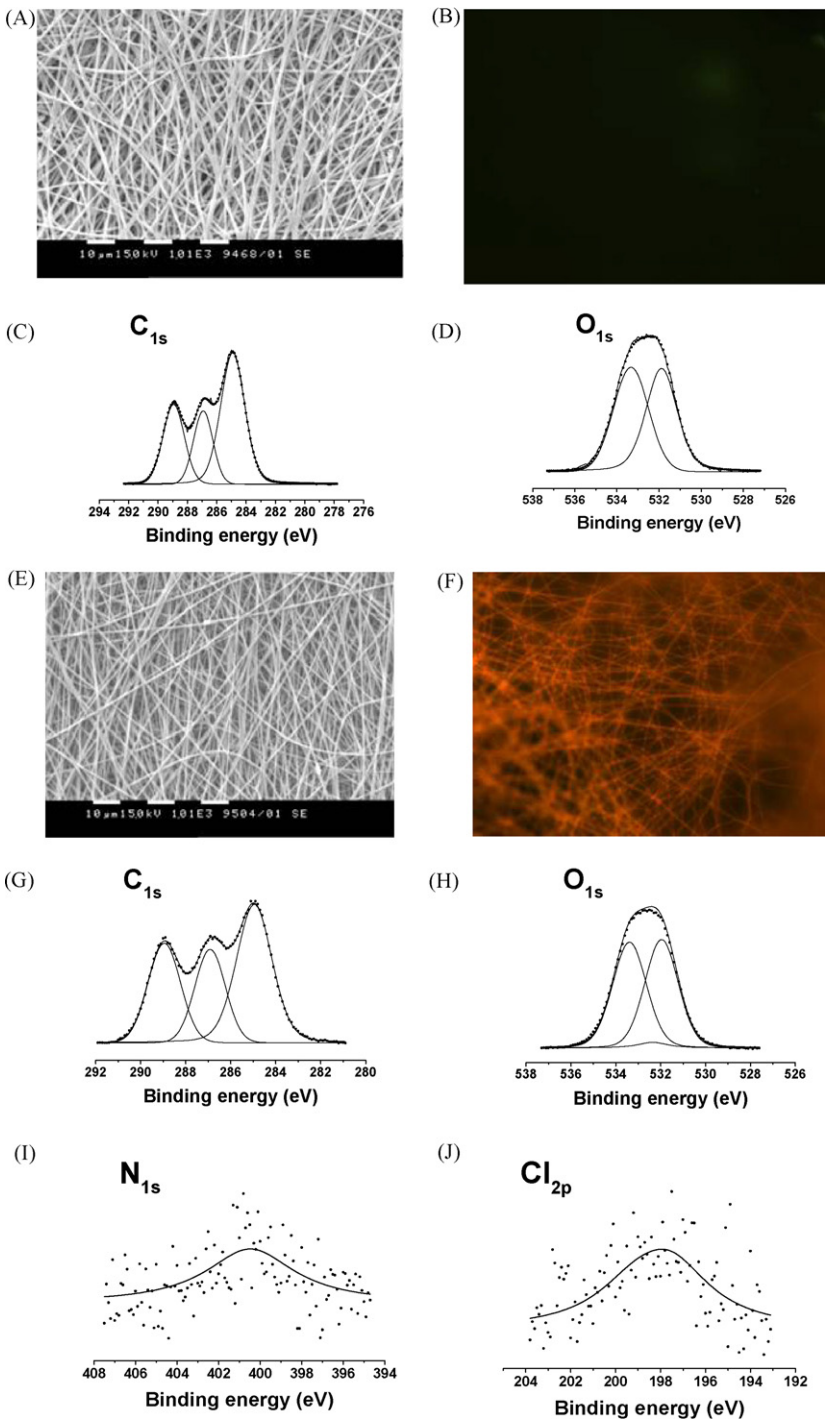

Fig. 3. SEM and fluorescence micrographs of fibrous implants: coPLA (A, B), coPLA/DOX (6 wt.% DOX) (E, F); magnification—×1000 (A, E) and ×40 (B, F). XPS peak fittings for implants of: coPLA [(C_{1s} (C) and O_{1s} (D)] and coPLA/DOX (6 wt.% DOX) [C_{1s} (G), O_{1s} (H), N_{1s} (I) and Cl_{2p} (J)].

detection of C_{1s}, O_{1s}, N_{1s} and Cl_{2p} (Fig. 3G–J) confirmed the successful incorporation of DOX in the surface of coPLA implants. In the expanded C_{1s} spectrum three peaks were identified (Fig. 3G). Considering the chemical structure of coPLA/DOX implant we could assign signals at 285 eV and 286.9 eV to the carbon in –C–H– and –C–C– of coPLA and in –C–H–, –C–C– and –C–N– of DOX and to the carbon in –C–O– of coPLA and in –C–OH, –C–OCH_3 and –C–O– of DOX, respectively. The peak at 288.9 eV is assigned to –O–C=O of coPLA and to –C–C=O and –O–C–O– of DOX. In the expanded O_{1s} spectrum of the coPLA/DOX implant, compared to that of the pristine implant, a new peak with a low intensity at 532.4 eV assigned to C–OH and –C–OCH_3 of DOX was observed (Fig. 3H). In the spectrum of the same implant a new peak corresponding to nitrogen was recorded at binding energy of 400.5 eV, which is assigned to $–NH_3^+$ of DOX (Fig. 3I). In addition, the spectrum of coPLA/DOX implant revealed the presence of Cl_{2p} peak at 198.0 eV (Fig. 3J). This peak is due to the presence of chlorine of the incorporated DOX.

The obtained results proved the successful preparation of nanofibrous implants containing physically entrapped model drug DOX. Since DOX possesses well-known high antitumor activity, the next step has been devoted to the assessment of the antitumor effi-

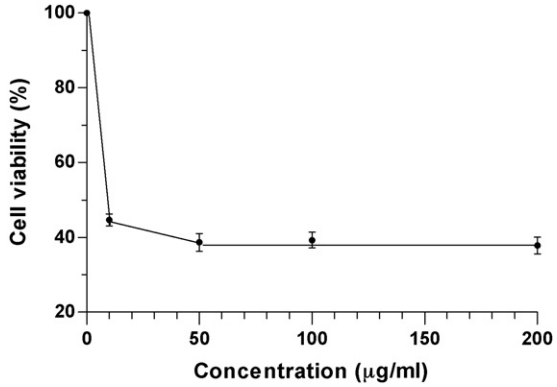

Fig. 4. Effect of DOX on the viability of the Graffi cells incubated in the presence of an increasing concentration of DOX for 24 h *in vitro*. The data are expressed as mean ± SD.

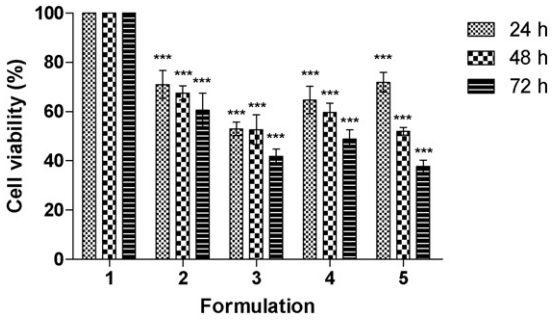

Fig. 6. Cell viability of Graffi tumor cells tested by MTT method after 24, 48 and 72 h of incubation with control–untreated Graffi tumor cells (1); QCh/coPLA implants with different QCh concentrations: 100 (2), 180 (3), and 300 μg/mL (4), and free DOX (10 μg/mL) (5). $^{***}p < 0.001$.

cacy of nanofibrous implants against Graffi myeloid tumor *in vitro* and *in vivo*.

3.2. Cytotoxic effects of DOX and DOX-containing implants on Graffi tumor cells

The cytotoxic effect of the anthracycline antitumor drug DOX against Grafi cells from hamsters was evaluated by MTT assay. As it can be seen in Fig. 4, DOX exerts an antiproliferative effect against Graffi cells. The IC_{50} value, which is the concentration required for 50% cell growth inhibition, is determined to be 10 μg/mL.

The viability of Graffi tumor cells (primary culture) cultured for 24, 48 and 72 h on the coPLA, QCh/coPLA, coPLA/DOX and QCh/coPLA/DOX implants was assessed by MTT assay. In this study, DOX was used as a positive control at a concentration of 10 μg/mL. Untreated Graffi cells were used as negative controls.

As seen in Fig. 5A, on the 24th h of incubation, the pristine and DOX-containing implants showed a high cytotoxicity against Graffi cells. With increasing the duration of the incubation period, the cytotoxic effect of the tested implants is manifested to a greater extent. The growth inhibition in Graffi cells was best pronounced on the 72nd hour of cultivation (Fig. 5C). The DOX-containing mats exhibited a high reduction in the Graffi cell viability (the viability of Graffi cells in the presence of coPLA/DOX and QCh/coPLA/DOX implants at 72nd h was decreased to 38.54 ± 2.46 and 38.08 ± 3.98, respectively). These implants manifested cytotoxicity similar to that of the free DOX.

The effect of various concentrations of QCh in the QCh/coPLA implants on the cytotoxicity against Graffi cells was evaluated as well (Fig. 6). With the prolongation of the incubation period and at higher QCh content, an increase of the inhibition of Graffi cell growth was observed. As shown in Fig. 6, the QCh/coPLA implants (concentration of QCh 180 μg/mL) showed the strongest effect on the reduction in the cell viability on the 72nd hour of incubation.

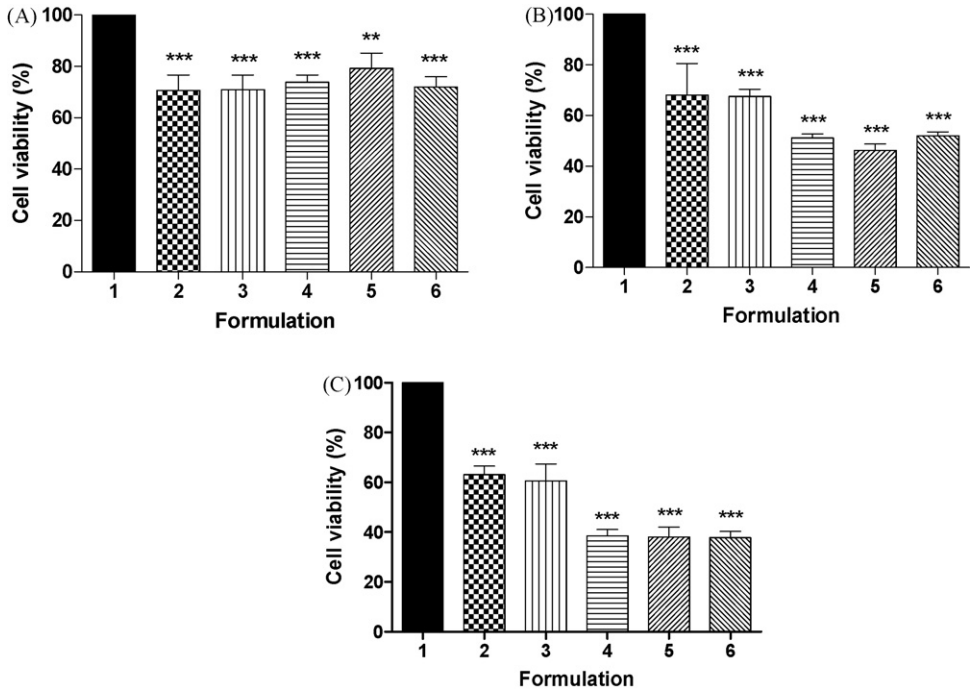

Fig. 5. Cell viability of Graffi tumor cells tested by MTT method after 24 h (A), 48 h (B) and 72 h (C) of incubation with different implants: control, untreated Graffi tumor cells (1); coPLA (2); QCh/coPLA (3); coPLA/DOX (4); QCh/coPLA/DOX (5); and free DOX (6). The total DOX content was 10 μg/mL; concentration of coPLA—233 μg/mL; concentration of QCh—100 μg/mL in the DOX-containing, coPLA-containing, and QCh-containing formulations, respectively. $^{***}p < 0.001$.

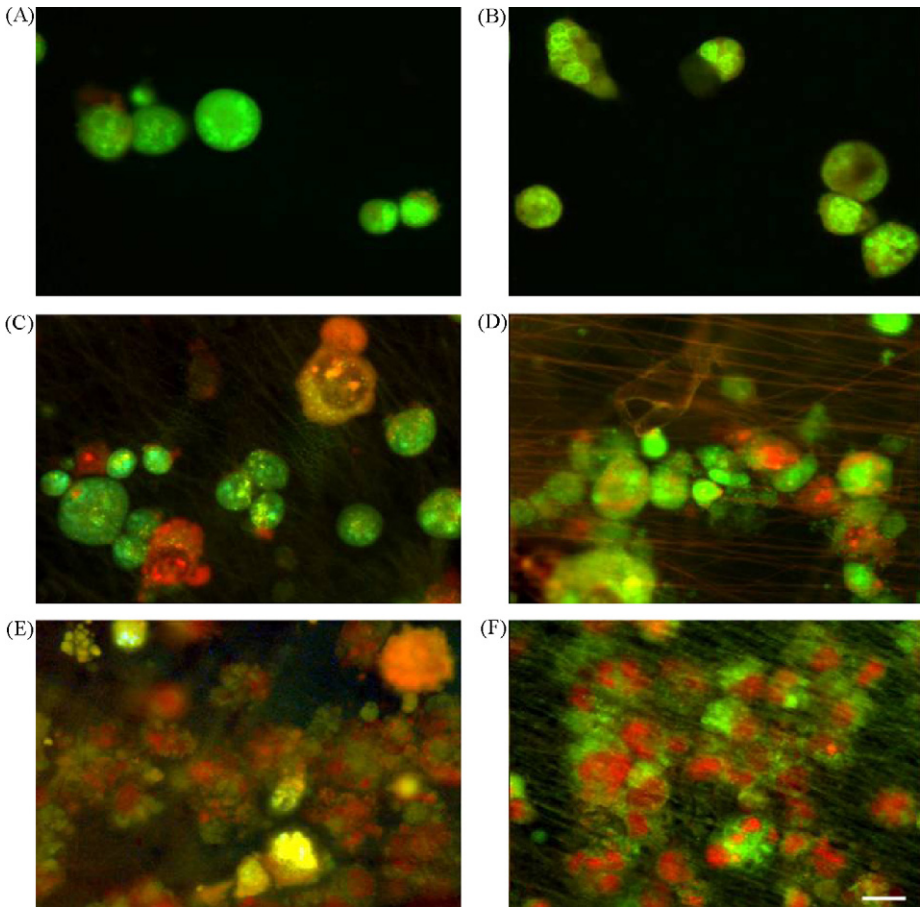

Fig. 7. Fluorescence microscopic visualization of morphological features of Graffi tumor cells, double-stained with AO and PI following 24 h incubation with free DOX and DOX-containing implants. Graffi tumor cells were cultured in RPMI 1640 medium with 10% bovine serum and maintained at 37°C and 5% CO_2: untreated Graffi cells (A); after incubation with DOX (B), and with implants: coPLA (C), QCh/coPLA (D), coPLA/DOX (E), QCh/coPLA/DOX (F). The total DOX content was 10 μg/mL; concentration of coPLA—233 μg/mL; concentration of QCh—100 μg/mL in the DOX-containing, coPLA-containing, and QCh-containing formulations, respectively.

3.3. Analysis of cell death by fluorescence microscopy

Experiments were carried out aimed to clarify whether inhibition of proliferation of Graffi tumor cells takes place through apoptosis. For this purpose Graffi cells were cultured for 24 h on the pristine and DOX-containing implants and then stained with AO and PI (DNA-fluorochromes). AO stains both viable and dead cells emitting strong green fluorescence, as a result of intercalation between the bases of double-stranded DNA and red-orange fluorescence after binding to single-stranded RNA (Han et al., 2008). In contrast, PI is a fluorochrome which does not stain viable cells with intact cell membrane. It stains the dead and late apoptotic cells with altered cell membrane permeability. Morphological changes in the Graffi tumor cells cultured on the different implants and processed with AO and PI were observed by fluorescence microscope (Fig. 7). The nucleus of the untreated Graffi cells showed homogenous fluorescence with no signs of segmentation and fragmentation. As shown in Fig. 7, nuclei with condensation of chromatin and apoptotic bodies (a typical sign of apoptosis) were observed in cells that had been in contact with DOX or DOX-containing implants. Microscopic observations showed that the QCh/coPLA implants also induce fragmentation of the nucleus of the Graffi cells. This effect is most clearly expressed in tumor cells cultured on coPLA/DOX and QCh/coPLA/DOX implants (Fig. 7E, F). The obtained results support the claim that QCh-based and DOX-containing implants induce death of Graffi tumor cells through apoptosis.

Quantitative assessment of apoptosis by the double staining method was performed. It was found that apoptotic Graffi cells cultured on coPLA/DOX and QCh/coPLA/DOX implants were 100% of all dead cells (Fig. 8). In the case of control free DOX this percentage was 92.62 ± 8.2%. The apoptotic cells incubated on QCh/coPLA and on coPLA implants were less than in other

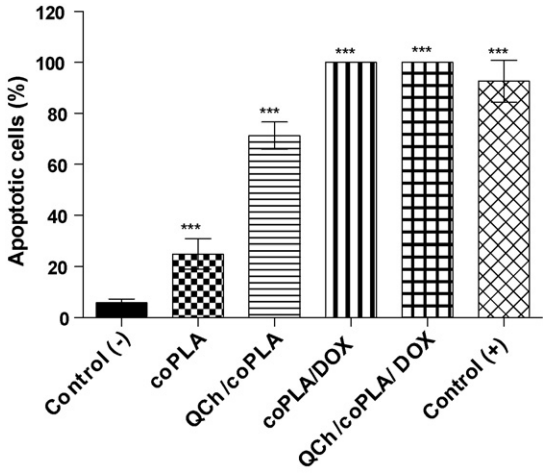

Fig. 8. Percentages of apoptotic Graffi cells after incubation on pristine and DOX-containing implants (DOX content was 10 μg/mL) for 24 h. Cells were cultured in DMEM and maintained at 37 °C and 5% CO_2. The data are representative of two independent experiments. The percentage of apoptotic cells was determined in more than 100 cells. *** $p < 0.001$.

formulations—71.29 ± 5.3% and 24.94 ± 1.5%, respectively. It is well known that the apoptotic processes underlying the immune defense mechanisms play an important role in tumor formation by elimination of damaged cells or cells with impaired proliferative activities. Hasegawa et al. (2001) showed that chitosan inhibits the growth of tumor cells by inducing apoptotic changes in bladder tumor cells. This inhibitory activity is due to the cytotoxic effect of chitosan in view of the fact that cells, treated with chitosan showed nuclear fragmentation and chromatin condensation—typical signs of the apoptotic cells. Other authors also have shown that chitosan induces apoptosis in promyelocytic leukemia cells (Pae et al., 2001). Some compounds of low molecular weights, possessing positively charged amino groups can selectively interact with the negatively charged mitochondria of the tumor cells, causing their death (Fantin et al., 2002). The antitumor activity of QCh-containing implants is most probably due to a similar mechanism. Another possible mechanism of action is inducing of apoptosis by engaging cell surface receptors. Since chitosan possesses positively charged tertiary amino groups, it can interact electrostatically with the negatively charged areas of the tumor cell membrane, inducing changes in their permeability. It has been reported that molecular iodine induces apoptosis in human breast carcinoma cells (Shrivastava et al., 2006). The possibility that the iodide anion of QCh contributes to the suppression of Graffi cell growth might not be ruled out.

3.4. *In vivo* antitumor efficacy of the implants

The *in vivo* antitumor efficacy of QCh-based and DOX-containing implants was studied in hamsters bearing experimental Graffi solid tumors. Two sets of experiments were carried out. In the first one after the operative intervention the implants were inserted intratumorally. Two groups of hamsters were used as controls: the first one was from tumor-bearing hamsters without any further intervention and the second one was from tumor-bearing hamsters injected intratumorally with free DOX.

The growth curves of Graffi tumors in hamsters followed-up for 20 days after intratumoral insertion of implants are shown in Fig. 9A. The tumor volume in the control group of non-treated hamsters bearing Graffi tumor increased rapidly (Fig. 9A, control). The coPLA implants did not impede the tumor growth. Free DOX showed superior antitumor effect to other formulations (by 20 days after injection the average tumor volume decreased and reached 10 400 mm^3). Significant antitumor effect in hamsters treated with QCh/coPLA, coPLA/DOX and QCh/coPLA/DOX implants was observed as well. By 20 days after insertion the average tumor volume in hamsters treated with QCh/coPLA implant had decreased and attained 22 000 mm^3. Previously, we have shown that DOX-containing QCh/coPLA nanofibrous mats are a matrix-type drug release system, which provides a sustained DOX release after an initial burst release (Ignatova et al., 2010). The observed significant reduction in tumor volume at the initial stage of tumor growth in the cases of QCh/coPLA/DOX and coPLA/DOX nanofibrous implants is consistent with the DOX release profile. For the sake of comparison, the average tumor volume in non-treated hamsters grew rapidly and reached 34 600 mm^3. The average tumor volume in hamsters treated intratumorally with coPLA/DOX or QCh/coPLA/DOX implants showed values similar to that observed for QCh/coPLA implant-treated hamsters—20 600 and 21 500 mm^3, respectively.

The reduction of the body weights of tumor-bearing hamsters after injection of DOX solution within 7 days compared to those of healthy hamsters was 17.2% (Fig. 9B). This significant decrease in body weights might be explained by the high toxicity of free DOX. Moreover, in the case of hamsters treated with free DOX, other signs of severe intoxication—abundant salivation, bare gums and teeth, protrusion of the tongue, prickly and fallen out hairs, exposed belly and blindness, were observed as well. The body weights of coPLA/DOX implant-treated hamsters decreased with 13.9%. For the same periods of time, the lowest body weight loss was found for QCh/coPLA and QCh/coPLA/DOX implants—7.8% and 4.3%, respectively. In these cases, the low toxicity could be accounted for by the biocompatibility and non-toxicity of the incorporated QCh in the former implants and by the sustained DOX release from implants (Ignatova et al., 2010). The symptoms of the severe toxicity in these two cases were not observed.

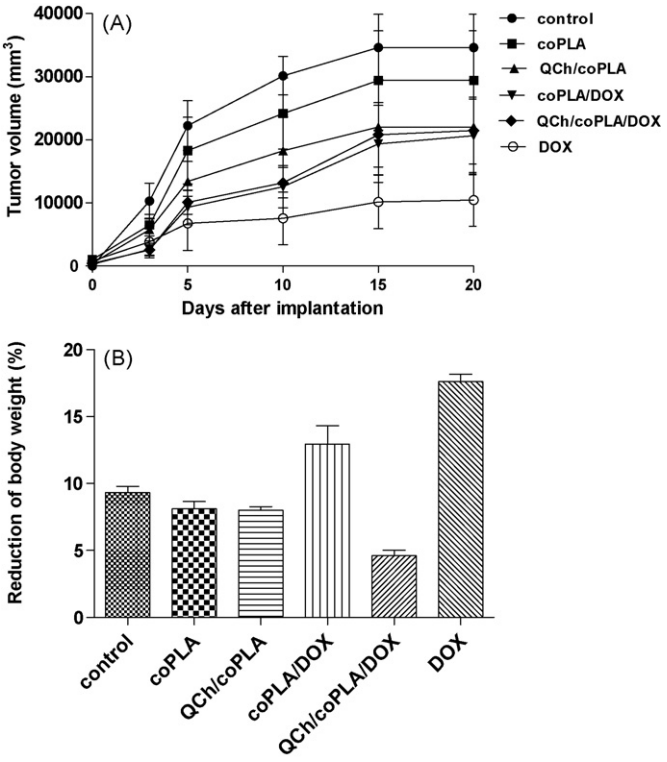

Fig. 9. Tumor volume changes (A) and reduction of body weight (in % of body weight of healthy hamsters) (B) of experimental and control hamsters bearing Graffi myeloid tumor after intratumoral insertion of nanofibrous implants on day 15. Reduction of body weight was determined 7 days after implantation. The total DOX content was 1.4 mg.

The survival rates of tumor-bearing hamster treated with implants with different composition are plotted on Fig. 10. In the case of hamsters treated with coPLA/DOX and QCh/coPLA/DOX implants 100% of the animals survived on the 20th day after the implantation. Approximately 80% and 60% of the animals survived in the other hamster groups and in the control hamster group, respectively. In the control group, as well as in the hamster groups treated with coPLA and QCh/coPLA implants 100% of the hamsters died on the 25th day. After the injection of free DOX and after the insertion of the DOX-containing implants 40% of the animals survived. It should be noted that between the 30th and 35th day 20% of the hamsters treated with coPLA/DOX and QCh/coPLA/DOX implants survived. Individual animals remained alive at least 90 days and at least 120 days after implantation in the cases of coPLA/DOX and QCh/coPLA/DOX implants, respectively. In the hamster group treated with free DOX, however, all the animals died within 30 days. The obtained results revealed that QCh/coPLA/DOX implants exhibited significant antitumor efficacy as well as low toxicity *in vivo*.

The histopathological studies of the tumor tissues were carried out on the 3rd and on the 7th day after the surgical intratumoral insertion of the nanofibrous implants. The studies revealed that the

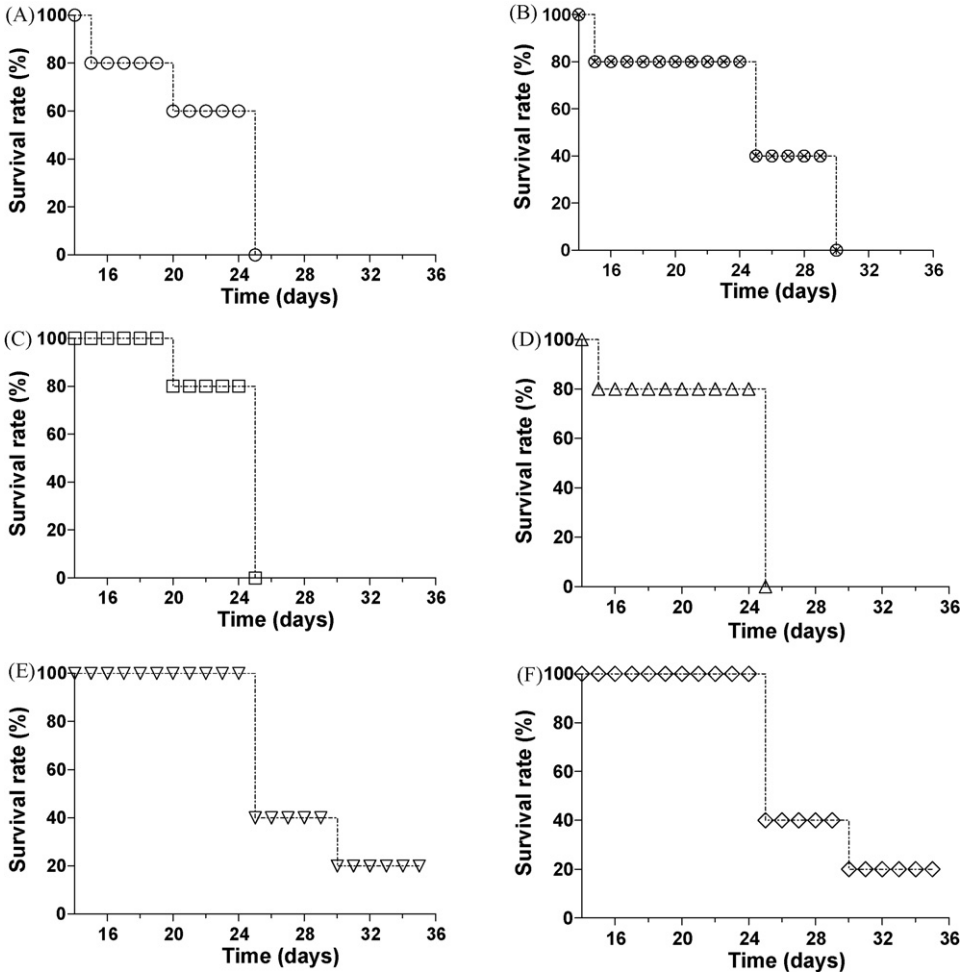

Fig. 10. Survival rates of experimental and control hamsters bearing Graffi myeloid tumor after intratumoral implantation on day 15: (A) control; (B) treated i.t. with DOX; (C) and with implants: coPLA; (D) QCh/coPLA (QCh:coPLA = 30:70, w/w); (E) coPLA/DOX and (F) QCh/coPLA/DOX (QCh:coPLA = 30:70, w/w). The total DOX content was 1.4 mg.

coPLA, QCh/coPLA, coPLA/DOX and QCh/coPLA/DOX implants led to a the following consecutiveness of the morphological changes in the zone around the implant: local haemorrhage – necrotic tumor cells (zone including cell detritus with nuclear fragmentation and disintegration or totally lytic cells as well as weakly acidophilic cells with a destroyed structure) – inflammatory zone (containing a large number of mononuclear cells and neutrophils with or without nuclear fragmentation) and finally a neoplastic tissue (Fig. 11). The present histopathological studies revealed that on the 3rd day after the implantation (Fig. 11B, a–c) a narrow zone of dead neoplastic tissue was observed around the QCh/coPLA implants (Fig. 11B, b). An entire destruction of the tumor was found around the QCh/coPLA/DOX implants (Fig. 11B, c). On the 7th day after the implantation (Fig. 11B, a^1–c^1) the most significant tissue killing effect was observed around the QCh/coPLA/DOX implant (Fig. 11B, c^1) and a less severe one around the QCh/coPLA implant (Fig. 11B, b^1). The tumor tissues with direct DOX inoculation were completely destroyed. Based on these findings it can be concluded that rapid destruction of small solid Graffi myeloid tumors can be performed using QCh/coPLA and QCh/coPLA/DOX implants. However, independently of the strong antitumor effects of the used nanofibrous implants containing QCh and DOX, viable neoplastic cells remained in the tumor periphery and they were a source for further Graffi myeloid tumor recurrences and metastases.

In the second set of experiments after surgical extirpation of the tumor, the implants (with different composition) were inserted in the same place. Two groups of hamsters served as controls – the first one of tumor-bearing animals with surgically removed tumor, and the second group – tumor-bearing animals without any further intervention. In the postoperative period the survival rate, the recurrence in the operative field, the appearance of metastases in regional lymph nodes, and the general status of operated and implanted hamsters compared to the control operated and non-operated hamsters were followed. The hamsters were examined on the 10th and the 15th day after implantation for recurrence in the operative field. It was found that recurrence occurred in all animals in the control groups, in the group of hamsters intratumorally injected with DOX and in the group of animals treated with coPLA implants. In contrast, on the 10th day of the insertion of the QCh/coPLA, coPLA/DOX and QCh/coPLA/DOX implants, the percentage of hamsters that exhibited recurrence was lower—83%, 50% and 60% respectively. In these cases the percentage of hamsters with recurrence remained almost unchanged on the 15th day after the implantation. For the group with coPLA/DOX implants the percentage of hamsters with recurrence increased to 83%. It should be noted that the highest survival rate was found in hamsters treated with QCh/coPLA/DOX implants (Fig. 12). In this case on the 35th day of implantation 40% of the hamsters were alive, whereas only 16% of the hamsters treated with QCh/coPLA implants survived. At the same time, in the other groups of hamsters 100% mortality was observed.

Photographs of hamsters at the third month after the placement of the QCh/coPLA and QCh/coPLA/DOX implants are shown in Fig. 13(A, B). During this period, the hamsters did not show any

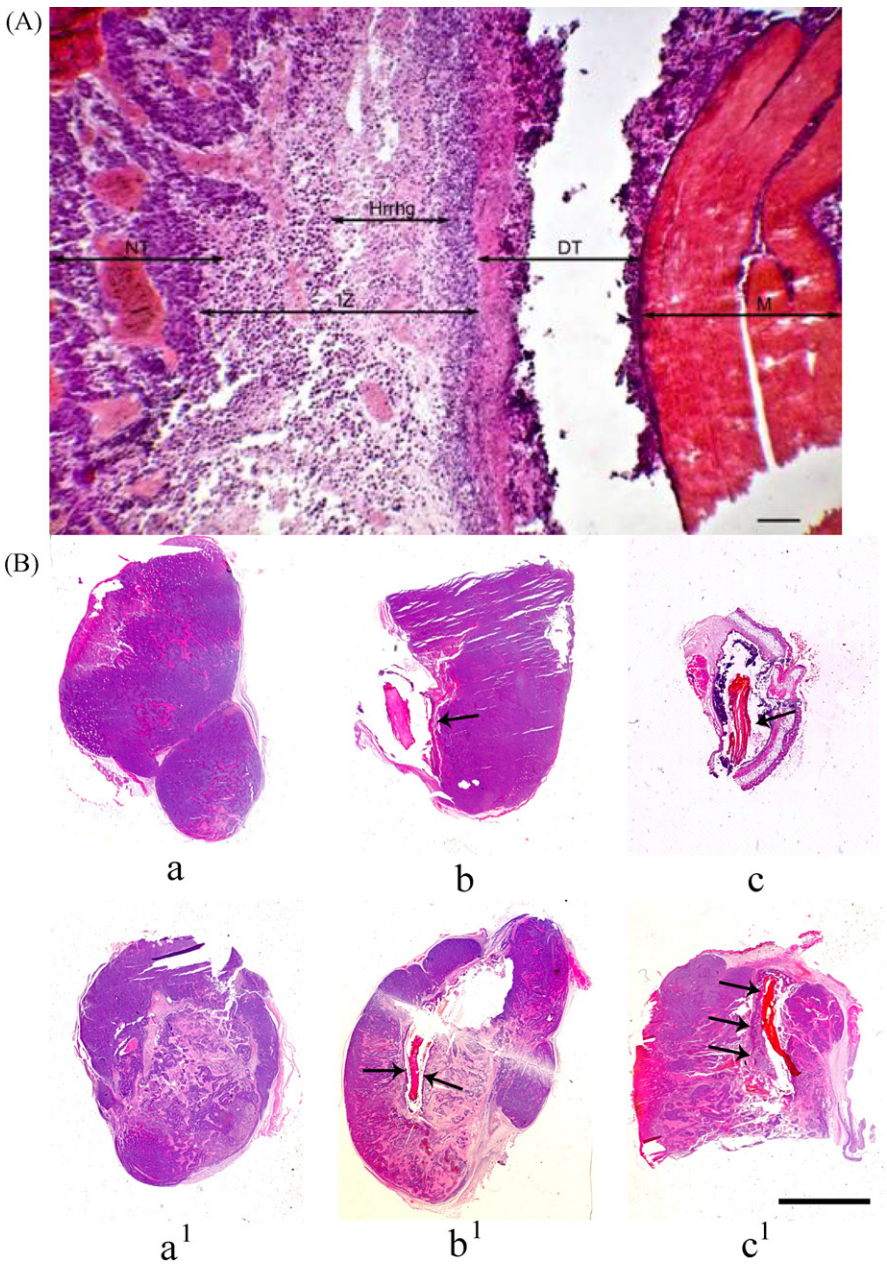

Fig. 11. (A) Histopathological changes around a QCh/coPLA implant in hamsters bearing Graffi myeloid tumor on day 7 after implantation: from right to left: implant (M), death tissue (DT), inflammatory zone (IZ), focal haemorrhages (Hrrhg), neoplastic tissue (NT). Paraffin section stained with haematoxylin–eosin. Bar = 300 μm; (B) Graffi tumor in hamsters on days 3 (a, b, c) and 7 (a^1, b^1, c^1) after implantation. (a, a^1) Graffi tumor-controls. Narrow zone of dead neoplastic tissue around the QCh/coPLA implant (b) and total dead tissues around a QCh/coPLA/DOX implant (c). Similar changes were found on the 7th day of nanofibrous implant insertion and a new neoplastic tissue grown in the tumor periphery is observed (b^1, c^1). Scannings of native histological preparations. Bar = 5 mm.

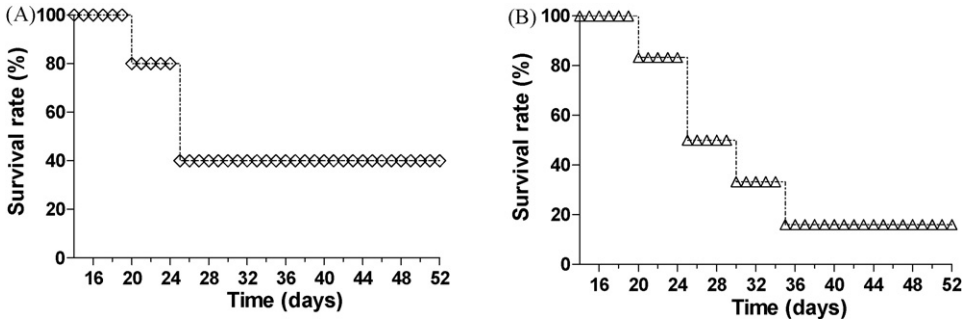

Fig. 12. Survival rates of hamsters bearing Graffi myeloid tumor after surgical tumor removal and subsequent placement of the implants in the operative field: (A) QCh/coPLA/DOX (QCh:coPLA = 30:70, w/w, DOX content was 1.4 mg) and (B) QCh/coPLA (QCh:coPLA = 30:70, w/w).

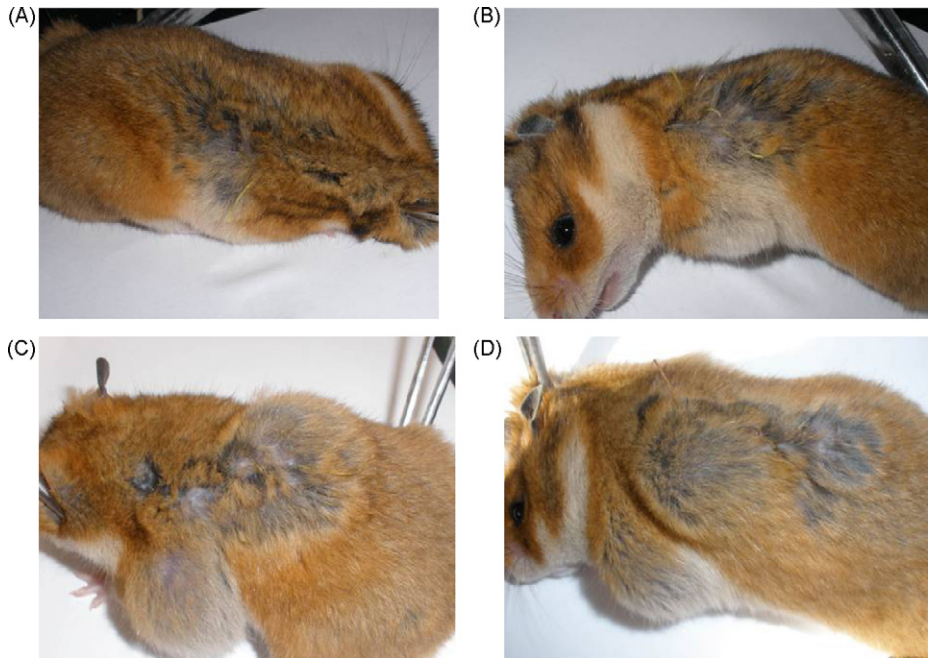

Fig. 13. (A, B) Photographs of hamsters (3 months after the operation) with no signs of recurrences, in which after tumor removal, the QCh/coPLA and QCh/coPLA/DOX implants were placed in the operative field; (C, D) photographs of hamsters with recurrences in the operative field and metastases in the regional lymph nodes.

clinical evidence of recurrence in the operative field and metastases in the regional lymph nodes. Their general health status was very good. They were with smooth and shiny hair, and the appearance and behavior of healthy hamsters. For the sake of comparison, the animals with recurrences in the operative field and metastases in the regional lymph nodes (20 days after tumor removal) are shown.

The results obtained in the first set of *in vivo* experiments revealed, that nanofibrous implants containing both QCh and DOX, showed suppression of the tumor volume and extension of the average survival time. Histopathological studies showed that local application of nanofibrous implants in the tumor induced the formation of zones with necrotic changes in the tumor tissue, and these areas of destruction were adjacent to the implant. In the periphery the tumor cells were preserved and that provided expansion of the intact tumor tissue and led to death of experimental animals as a result of progressive development of the tumor.

In the experiments with QCh/coPLA and QCh/coPLA/DOX implants locally inserted in the place of the removed tumor an increase in the survival rate and a lower rate of recurrence in the operative field and metastases in regional lymph nodes were found. In the control animals injected with free DOX toxicity was observed while the incorporation of DOX in QCh/coPLA implants did not lead to abnormalities in the health status and the development of the experimental animals.

4. Conclusion

The present study demonstrates that when formulated as a nanofibrous implant, the antitumor efficacy of DOX can be significantly increased and the side effects can be reduced when it is used together with quaternized chitosan (QCh), most likely because of a synergistic action of DOX and QCh. The QCh-based and DOX-containing nanofibrous implants significantly reduced the Graffi cell viability and their *in vitro* antitumor efficacy was similar to that of free DOX. The observed effect was mainly due to induction of apoptosis in the cells. The local application of the implants containing both QCh and DOX in the tumor tissue showed high antitumor efficacy *in vivo* and was better tolerated as compared to free DOX. The experiments in which the QCh/coPLA/DOX implants were inserted locally into the tumor site postoperatively after the tumor extirpation, showed a decrease of the percentage of recurrence in the operative field and of metastases in the regional lymph nodes and an increase of the animal survival rate. Therefore, this type of nanofibrous implants may be considered promising as drug delivery system for local application in the treatment of solid tumors.

Acknowledgements

Financial support from the Bulgarian National Science Fund (Grant DO-02-164/2008) is gratefully acknowledged.

References

Cho, Y.I., Park, S., Jeong, S.Y., Yoo, H.S., 2009. *In vivo* and *in vitro* anti-cancer activity of thermo-sensitive and photo-crosslinkable doxorubicin hydrogels composed of chitosan–doxorubicin conjugates. Eur. J. Pharm. Biopharm. 73, 59–65.

Crown, J., Dieras, V., Kaufmann, M., von Minckwitz, G., Kaye, S., Leonard, R., Marty, M., Misset, J.-L., Osterwalder, B., Piccart, M., 2002. Chemotherapy for metastatic breast cancer-report of a European expert panel. Lancet Oncol. 3, 719–727.

Fantin, V.R., Berardi, M.J., Scorrano, L., Korsmeyer, S.J., Leder, P., 2002. A novel mitochondriotoxic small molecule that selectively inhibits tumor cell growth. Cancer Cell 2, 29–42.

Freedman, R.S., Herson, J., Wharton, J.T., Rutledge, F.N., 1980. Single-agent-chemotherapy for recurrent carcinoma of the cervix. Cancer Clin. Trials 3, 345–350.

Han, H.D., Song, C.K., Park, Y.S., Noh, K.H., Kim, J.H., Hwang, T., Kim, T.W., Shin, B.C., 2008. A chitosan hydrogel-based cancer drug delivery system exhibits synergistic antitumor effects by combining with a vaccinia viral vaccine. Int. J. Pharm. 350, 27–34.

Hasegawa, M., Yagi, K., Iwakawa, S., Hirai, M., 2001. Chitosan induces apoptosis via caspase-3 activation in bladder tumor cells. Jpn. J. Cancer Res. 92, 459–466.

Hu, F.-Q., Liu, L.-N., Du, Y.-Z., Yuan, H., 2009. Synthesis and antitumor activity of doxorubicin conjugated stearic acid-g-chitosan oligosaccharide polymeric micelles. Biomaterials 30, 6955–6963.

Huang, R., Mendis, E., Rajapakse, N., Kim, S.-K., 2006. Strong electronic charge as an important factor for anticancer activity of chitooligosaccharides (COS). Life Sci. 78, 2399–2408.

Ignatova, M.G., Manolova, N.E., Toshkova, R.A., Rashkov, I.B., Gardeva, E.G., Yossifova, L.S., Alexandrov, M.T., 2010. Electrospun nanofibrous mats containing quaternized chitosan and polylactide with in vitro antitumor activity against HeLa cells. Biomacromolecules 11, 1633–1645.

Ignatova, M., Manolova, N., Markova, N., Rashkov, I., 2009. Electrospun non-woven nanofibrous hybrid mats based on chitosan and PLA for wound-dressing applications. Macromol. Biosci. 9, 102–111.

Ignatova, M., Manolova, N., Rashkov, I., 2007. Novel antibacterial fibers of quaternized chitosan and poly(vinyl pyrrolidone) prepared by electrospinning. Eur. Polym. J. 43, 1112–1122.

Ignatova, M., Starbova, K., Markova, N., Manolova, N., Rashkov, I., 2006. Electrospun nano-fibre mats with antibacterial properties from quaternised chitosan and poly(vinyl alcohol). Carbohydr. Res. 34, 2098–2107.

Janes, K.A., Fresneau, M.P., Marazuela, A., Fabra, A., Alonso, M.J., 2001. Chitosan nanoparticles as delivery systems for doxorubicin. J. Controlled Release 73, 255–267.

Jun, Z., Hou, H., Schaper, A., Wendorff, J., Greiner, A., 2003. Poly-L-lactide nanofibers by electrospinning—influence of solution viscosity and electrical conductivity on fiber diameter and fiber morphology. e-Polymers no. 009, 1–9.

Kim, C.H., Choi, J.W., Chun, H.J., Choi, K.S., 1997. Synthesis of chitosan derivatives with quaternary ammonium salt and their antibacterial activity. Polym. Bull. 38, 387–393.

Liu, L., Li, C.X., Li, X.C., Yuan, Z., An, Y.L., He, B.L., 2001. Biodegradable polylactide/poly(ethylene glycol)/polylactide triblock copolymer micelles as anticancer drug carriers. J. Appl. Polym. Sci. 80, 1976–1982.

Mincheva, R., Paneva, D., Manolova, N., Rashkov, I., 2005. Preparation of polyelectrolyte-containing nanofibers by electrospinning in the presence of a non-ionogenic water-soluble polymer. J. Bioact. Compat. Polym. 20, 419–435.

Mossmann, T., 1983. Rapid colorimetric assay for cellular growth and survival: application to proliferation and cytotoxicity assays. J. Immunol. Methods 65, 55–63.

Pae, H.O., Seo, W.G., Kim, N.Y., Oh, G.S., Kim, G.E., Kim, Y.H., Kwak, H.J., Yun, Y.G., Jun, C.D., Chung, H.T., 2001. Induction of granulocytic differentiation in acute promyelocytic leukemia cells (HL-60) by watersoluble chitosan oligomer. Leuk. Res. 25, 339–346.

Park, J.H., Saravanakumar, G., Kim, K., Kwon, I.C., 2010. Targeted delivery of low molecular drugs using chitosan and its derivatives. Adv. Drug Deliv. Rev. 62, 28–41.

Prahalathan, C., Selvakumar, E., Varalakshmi, P., 2006. Lipoic acid modulates adriamycin induced testicular toxicity. Reprod. Toxicol. 21, 54–59.

Qin, C., Du, Y., Xiao, L., Li, Z., Gao, X., 2002. Enzymic preparation of water-soluble chitosan and their antitumor activity. Int. J. Biol. Macromol. 31, 111–117.

Rabea, E.I., Badawy, M.E.T., Christian, V., Stevens, C.V., Smagghe, G., Steurbaut, W., 2003. Chitosan as antimicrobial agent: applications and mode of action. Biomacromolecules 4, 1454–1465.

Ranganath, S.H., Wang, C.-H., 2008. Biodegradable microfiber implants delivering paclitaxel for post-surgical chemotherapy against malignant glioma. Biomaterials 29, 2996–3003.

Rasband, W.S., 1997–2006. ImageJ. U. S. National Institute of Health, Bethesda, Maryland, USA, http://rsb.info.nih.gov/ij/.

Reneker, D.H., Chun, I., 1996. Nanometre diameter fibers of polymer, produced by electrospinning. Nanotechnology 7, 216–223.

Shrivastava, A., Tiwari, M., Sinha, R.A., Kumar, A., Balapure, A.K., Bajpai, V.K., Sharma, R., Mitra, K., Tandon, A., Godbole, M.M., 2006. Molecular iodine induces caspase-independent apoptosis in human breast carcinoma cells involving mitochondria-mediated pathway. J. Biol. Chem. 281, 19762–19771.

Spasova, M., Manolova, N., Paneva, D., Rashkov, I., 2004. Preparation of chitosan-containing nanofibres by electrospinning of chitosan/poly(ethylene oxide) blend solutions. e-Polymers no. 056, 1–12, www.e-polymers.org.

Spasova, M., Mincheva, R., Paneva, D., Manolova, N., Rashkov, I., 2006. Perspectives On: criteria for complex evaluation of the morphology and alignment of electrospun polymer nanofibers. J. Bioact. Compat. Polym. 21, 465–479.

Toshkova, R., Krasteva, I., Nikolov, S.D., 2008. Immunorestoration and augmentation of mitogen lymphocyte response in Graffi tumor bearing hamsters by purified saponin mixture from Astragalus corniculatus. Phytomedicine 15, 876–881.

Wahab, S.I.A., Abdul, A.B., Alzubairi, A.S., Elhassan, M.M., Mohan, S., 2009. In vitro ultramorphological assessment of apoptosis induced by zerumbone on (HeLa). J. Biomed. Biotechnol., 1–10, doi:10.1155/2009/769568, Article ID 769568.

Xiangyang, X., Ling, L., Jianping, Z., Shiyue, L., Jie, Y., Xiaojin, Y., Jinsheng, R., 2007. Preparation and characterization of *N*-succinyl-*N'*-octyl chitosan micelles as doxorubicin carriers for effective anti-tumor activity. Colloids Surf. B 55, 222–228.

Xu, X., Chen, X., Xu, X., Lu, T., Wang, X., Yang, L., Jing, X., 2006. BCNU-loaded PEG–PLLA ultrafine fibers and their in vitro antitumor activity against Glioma C6 cells. J. Controlled Release 114, 307–316.